Int j simul model 23 (2024) 1, 89-100
Original scientific paper

GENETIC LAW OF THICKNESS DISTRIBUTION OF STRIP STEEL DURING HOT ROLLING PROCESS

Yin, B. L.[*,**]; Cui, X. Y.[*]; Elmi, S. A.[*]; Li, Z. Z.[*]; An, H. L.[***] & Bai, Z. H.[*,****,#]
[*] National Engineering Research Center for Equipment and Technology of Cold Strip Rolling, Yanshan University, Qinhuangdao 066004, China
[**] Tangshan Iron and Steel Group Co., Ltd., Tangshan 063000, China
[***] HBIS Materials Technology Research Institute, HBIS Group, Shijiazhuang 050023, China
[****] State Key Laboratory of Metastable Materials Science and Technology, Yanshan University, Qinhuangdao 066004, China
E-Mail: bai_zhenhua@aliyun.com ([#] Corresponding author)

Abstract
To solve the common issue of transverse thickness variation in finished strip steel during the seven-stand hot continuous rolling process, the deformation of rolls in the rolling process of beam Steel 700L and the genetic characteristics of plate thickness distribution were analysed by finite element simulation. Using actual process parameters from the production of beam Steel 700L, a dynamic rolling finite element model was established. The equivalent stress field between the working rolls and strip steel in each stand and the exit thickness distribution of beam Steel 700L were investigated. Results show that the equivalent stress indicates a gradual increase despite a decreasing reduction rate during rolling. Deviations in thickness between the centre and edges of the strip steel at the exit of each stand become apparent from the second stand onwards, demonstrating a hereditary phenomenon during the rolling process. A comparison of measured and simulated thickness reveals errors within 5 %, validating the accuracy of the simulation. The obtained findings provide a foundational understanding for addressing thickness defects in subsequent beam Steel 700L production.
(Received in September 2023, accepted in January 2024. This paper was with the authors 1 month for 2 revisions.)

Key Words: Seven Stands, Hot Continuous Rolling, Thickness Distribution, Finite Element

1. INTRODUCTION

Strip steel, constituting approximately 45 % of total steel production, plays a pivotal role in various industries such as automotive, shipbuilding, bridges, construction, and household appliances. The increasing demands for high-quality strip steel products, driven by rapid developments in automotive, defence, and household appliance industries, underscore the significance of technological advancements in strip steel production [1]. The technological proficiency of strip steel production and its proportion in the rolling process serve as key indicators of a country's steel production development [2]. In the pursuit of market competitiveness, domestic steel enterprises consistently expand their hot rolling product catalogues to encompass high-value-added products like high-grade pipeline steel, electrical silicon steel, automotive cold-rolled panels, and tin-plated coating plates [3]. Thickness precision is a critical quality indicator for strip steel, directly influencing both strip product yield and the quality of subsequent deep-processed products. As scientific and technological advancements progress, thickness control has evolved into a core technology in strip steel production [4].

The seven-stand hot continuous rolling mill significantly improves the precision control of thickness distribution and surface quality of strip steel. However, challenges persist in achieving transverse thickness uniformity, particularly in the production of high-quality strip steel. This challenge, known as transverse thickness deviation, adversely impacts product quality, necessitating downgrading and affecting mill production efficiency. Additionally,

thickness deviation significantly affects downstream processes, potentially causing strip misalignment and breakage, resulting in substantial losses for the mill.

With the growing demand for higher quality strip steel, the allowable range for transverse thickness deviation has decreased. Consequently, some experts in the metallurgical field are increasingly focusing on research related to thickness control. While numerical simulation of hot rolling results has seen advancements in precision with the development of computer technology [5], limited research directly studies the evolution of strip steel thickness distribution throughout the entire hot rolling process using numerical simulation. For instance, Schindler et al. [6] utilized the finite element method to simulate operational issues in the hot rolling process of wide and thick products. Chai et al. [7] employed the finite element method to solve unknown metal transverse flow variables, analysing and comparing flatness and longitudinal residual stress evolution in the rolling process of thick and thin plates using a flatness calculation model. In terms of thickness control for strip steel, common practices involve force analysis, mathematical model establishment, and targeted improvements in rolling parameters and rolling process parameters [8, 9]. However, using formulaic methods may not effectively address thickness evolution during the hot continuous rolling process with seven stands.

This study aims to provide directions for the control of transverse thickness deviation in hot-rolled strip steel, addressing an essential area requiring further investigation and resolution in the field of hot rolling thickness control. Using various finite element softwares, this study leverages the significant advantages of Marc software in solving three-dimensional large deformation thermo-elastic-plastic problems for finite element simulation analysis.

2. STATE OF THE ART

The investigation into the transverse thickness distribution of strip steel can be broadly categorized into two main areas: studies on thickness prediction during the rolling process and research on thickness control technologies. Existing literature in these domains has provided valuable insights into the genetic laws governing transverse thickness distribution during the seven-stand hot continuous rolling process examined in this study.

In the exploration of thickness prediction techniques during the rolling process, Liu et al. [10] utilized optimization algorithms, including machine learning and neural networks, to predict the thickness, profile, and flatness of hot-rolled strip steel. Their methods accurately predicted the transverse thickness distribution and pre-tension transverse distribution of the final product strip steel. However, despite achieving high prediction accuracy, these methods did not offer insights into the evolving transverse thickness distribution at the exit of each stand during the rolling process. Liu and Xiao [11] focused on determining the minimum rollable thickness of strip steel, establishing a theoretical calculation model based on Fleck's theory for the production of ultra-thin strip steel. Although they defined product specifications and rolling rules for existing mills and determined roller diameter and force and energy parameters for mill design, they did not propose a method for predicting transverse thickness distribution. Gu et al. [12] identified rolling force settings as a major cause of thickness deviation in strip steel. Through measures such as improving the uniformity of strip steel temperature and optimizing thickness-setting models, including AGC head response, they enhanced the accuracy of product flatness.

In the realm of research on thickness control of finished strip steel, Ma et al. [13] discovered a quadratic nonlinear relationship between the transverse thickness difference of cold-rolled strip steel and the wedge and crown of hot-rolled strip steel. They suggested that reducing the edge drop of hot-rolled strip steel is beneficial for suppressing the transverse thickness difference of cold-rolled strip steel, although they did not analyse the effectiveness of this

approach in practical applications. Hu et al. [14] proposed an optimal tension and thickness control method based on the Reverse Horizontal Control (RHC) strategy, exhibiting excellent tracking performance and strong constraint-handling capabilities. Zeng et al. [15] utilized neural network simulation to establish a transverse thickness prediction model for strip steel and developed a model-free controller for thickness control. Liu et al. [16] established an F7 exit wedge closed-loop feedback control model based on finite element modelling and the relationship between the inclination pressure and exit wedge shape on both sides of the rolling mill.

The aforementioned research outcomes primarily focus on individual aspects of either thickness prediction or thickness control during the rolling process. Moreover, their connection to actual on-site production is limited, especially concerning the evolutionary patterns of transverse thickness distribution during the seven-stand hot continuous rolling process and the insufficiently explored study on the control of thickness deviation defects. In this study, the genetic characteristics of the transverse thickness distribution of 700L beam steel was investigated by finite element simulation in a seven-stand hot continuous rolling mill unit as it passed through each stand. A dynamic rolling finite element model was established based on actual field data, obtaining the equivalent stress field between the working rolls of each stand and the strip steel by applying constraints. Simultaneously, the transverse thickness distribution of the strip steel at the exit of each stand was obtained to reveal the genetic laws of transverse thickness distribution during the seven-stand hot continuous rolling process. Based on this, the rolling process parameters to address thickness deviation defects were adjusted, and after application in on-site production, the defects of transverse thickness deviation in the finished strip steel were successfully resolved.

The remaining sections of this study are organized as follows. Section 3 describes the actual operating conditions of the seven-stand hot continuous rolling mill unit and establishes a finite element model of the rolling process. In section 4, we calculate the stress distribution state in the deformation zone during the rolling process, the transverse thickness distribution of strip steel at the exit of each stand, and the on-site application of optimized rolling process parameters. The final section summarizes the results and provides relevant conclusions.

3. METHODOLOGY

By discretizing the mesh of the rolling element and constructing a dynamic finite element model for rolling, the groundwork is established for simulating the rolling process.

3.1 Model parameter configuration

To accurately study the deformation of the roll system, it is necessary to establish a three-dimensional rolling model for simulation analysis. During the three-dimensional rolling process, the changes in the roll system are represented by the bending deformation of the roll axis. Obtain the equipment and rolling process parameters of the seven stand hot rolling mill to determine the material properties of the established finite element model of the rolling mill. At the same time, select the rolled piece as an elastic-plastic material, and the specific parameters are shown in Table I.

Table I: Model parameter table.

Support roller diameter (mm)	1500	Support roller body length (mm)	3300
Work roll diameter (mm)	750	Work roll body length (mm)	3300
Elastic modulus of work roll (MPa)	210000	Poisson’s ratio of work rolls	0.30
Material	Beam steel 700L	Yield limit (MPa)	204.6

3.2 Unit grid division

Steps: Create a two-dimensional model of the rolling mill in CAD, convert the format, and import it into Marc software for grid partitioning. When dividing the mesh between the work roll and the support roll, considering the larger volume of the roll and the fewer actual contact positions, in order to reduce the number of units and facilitate calculation, the contact position units between the support roll and the work roll, and between the work roll and the strip steel are divided more densely, while other positions are relatively sparse [17, 18]. This can improve calculation efficiency while ensuring simulation accuracy. At the same time, the following principles should be ensured during grid partitioning:

(1) Due to the fact that triangular meshes are prone to distortion at vertices, which has a significant impact on the calculation results, all meshes are divided into four node quadrilateral meshes during modelling.

(2) The subdivision of the mesh in the contact area adopts a one-third division method, which can ensure that the mesh of the roller remains consistent in the contact area, thereby ensuring the calculation accuracy during the calculation process.

(3) On the circumference where the support roller contacts the work roller and the work roller contacts the rolled piece, considering the convergence problem of future contact analysis calculations, the grid division of the outer circumference should be as consistent as possible with the grid density of the rolled piece. Then, the grid density gradually increases from the centre to the outer circumference, forming an outer dense and inner sparse grid, effectively reducing the number of grids while ensuring calculation accuracy.

When dividing the work roll into grids, taking into account the actual assembly situation and the length of the rolled sheet, ensure that the length of the encrypted arc is equal to the length of the rolled sheet. Obtain the mesh division model of the rolling mill as shown in Fig. 1. Due to the dense grid division in the contact area, the black part is presented in Fig. 1 [19].

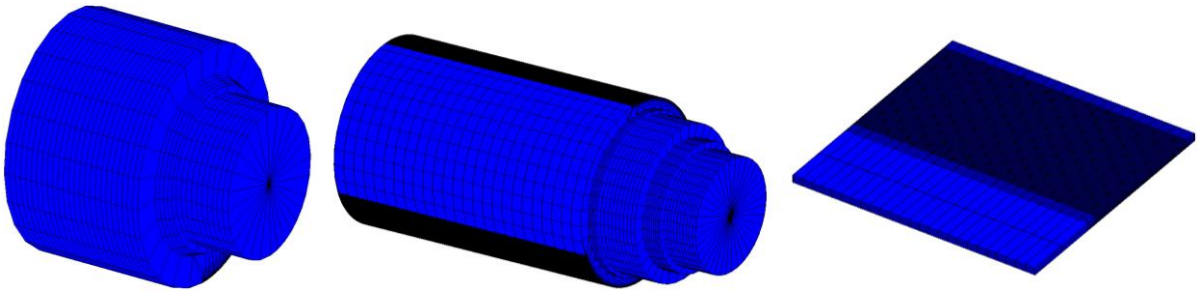

a) b) c)

Figure 1: Mesh partitioning model for rolling mill; a) support roller grid unit; b) work roller grid unit; c) strip steel grid element.

The overall layout and mesh division finite element model between the support roller and the work roller, as well as between the work roller and the strip, are shown in Fig. 2. In order to rotate the support roller and work roller around their respective axes, it is necessary to enable the large displacement option in the analysis options. By sticking them together through contact with the rigid body, the rotation of the rigid body is used to drive the rotation of the elastic roller. In this model, the driving roller is the work roller, which drives the support roller to rotate through friction. The friction force between the work roll and the rolled part drives the movement of the rolled part.

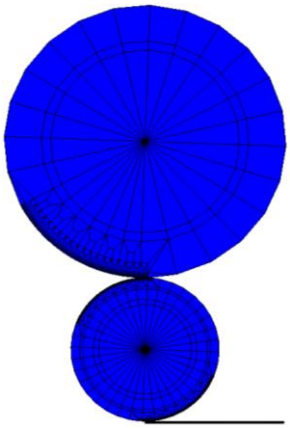

Figure 2: Overall grid model of rolling mill.

3.3 Definition of other boundary conditions

The constraints on the support roller in the model are to limit the displacement of the main control point of the support roller in the *x*- and *y*-directions, set the pressure in the *y*-direction, and limit the rotation in the *y*-direction. Limit the displacement and rotation of the main control point of the work roll in the *x*-direction and the *y*-direction, and give the rotation arc of the work roll in the *z*-direction.

At the same time, the middle cross-section of the support roll and the work roll body is symmetrically treated, and the displacement in the *x*-direction of all rolls in the roll system is fixed to prevent the impact of roll left and right deviation through simulation analysis. Apply front and rear tension to the plate to make it straight during the rolling process, achieving the function of a coiler. The grid in the contact area between the work roller and the strip is shown in Fig. 3. It is difficult to simulate the conveying and biting process of the plate and belt in the calculation, therefore, simplification has been made in the calculation. The simplified method is to first place the rolled piece into the roll gap, then give a pressure displacement to the support roll, and then drive the work roll to rotate to drive the rolled piece for rolling.

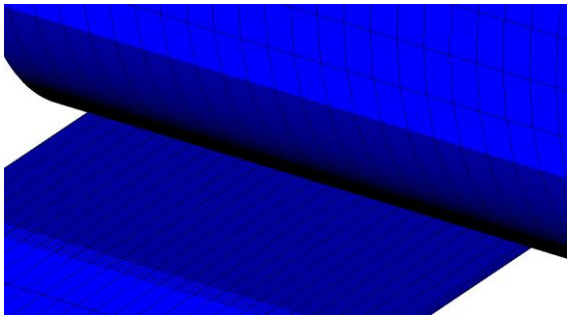

Figure 3: Mesh in the contact area between work rolls and strip steel.

3.4 Establishment of dynamic rolling finite element model

Based on the equipment and process characteristics of the 2060 seven-stand hot rolling mill, a nonlinear finite element Marc was used to establish a finite element analysis model for the seven stand hot rolling process. Considering the computational complexity, the rolls of each rack will be indented to improve the calculation speed. The spacing is 160 mm, which is much longer than the length of the deformation zone. The rollers are all elastic bodies, and the rolled parts are elastic-plastic bodies.

It is difficult to simulate the conveying and biting process of the plate and belt in the calculation, therefore, simplification has been made in the calculation. The simplified method

is to first place the rolled piece into the roll gap, then give a pressure displacement to the support roll, and then drive the work roll to rotate to drive the rolled piece for rolling. The calculation results only analyse the steady-state rolling state.

In this model, the driving roller is the work roller, which drives the support roller to rotate through friction. The friction between the work roller and the rolled piece drives the movement of the rolled piece. Among them, the rollers are treated as elastomers and rotate around the axis. Based on refining the finite element mesh of the rolling mill, simplifying the calculation, and treating the elastic bodies of the support and work rolls, a seven-stand hot continuous rolling finite element model was established, as shown in Fig. 4.

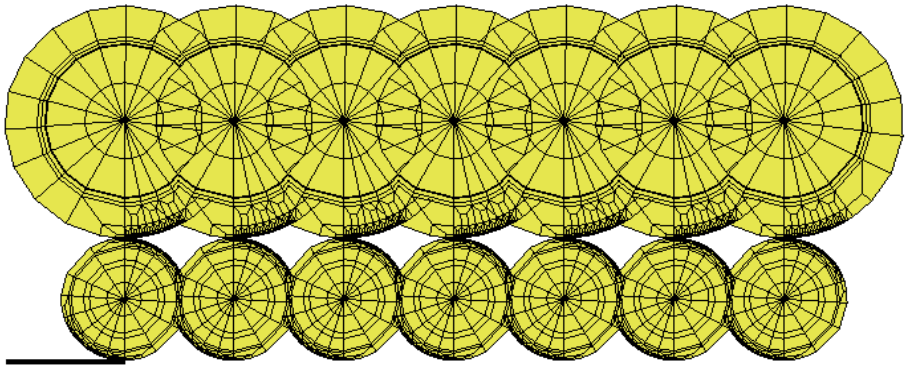

Figure 4: Finite element model of seven stand hot continuous rolling.

4. RESULT ANALYSIS AND DISCUSSION

Simulate the deformation process of the 700L beam steel during 7 rolling passes and record the thickness distribution of the rolled pieces at the outlet of each stand during the rolling process.

Table II displays the process parameters and parameters of the rolled pieces for the 2060 hot continuous rolling mill when rolling 700L beam steel. The incoming material has a thickness of 46.17 mm and a width of 1535 mm, while the measured final rolling outlet thickness is 5.06 mm. The rolled strip steel corresponds to the actual steel grade used in production, specifically, product 3 of 700L beam steel.

Table II: Rolling process parameters.

Rack number	**1#**	**2#**	**3#**	**4#**	**5#**	**6#**	**7#**
Outlet thickness (mm)	27.52	16.79	11.55	8.66	6.69	5.62	5.06
Reduction rate (%)	40.4	39	31.2	25	22.7	16	10
Rolling force (kN)	21094	22206	19985	17765	14434	12879	11104
Work roll bending force (kN)	600	600	600	600	650	650	650
Work roll displacement (mm)	10	10	10	10	10	10	10
Friction coefficient	0.3	0.3	0.3	0.3	0.3	0.3	0.3
Tension (MPa)	483	572	668	751	851	981	981
Deformation resistance (MPa)	151.7	190.5	223.7	257	318.2	329	361

4.1 Stress distribution status in deformation zone during rolling process

In accordance with Table II, which details the rolling process parameters, configure the following parameters within the Marc software: reduction for each pass, bending force applied to the work roll, material properties and deformation resistance of the strip steel, initial temperature, and tension before and after rolling. Ensure that corresponding initial and boundary conditions are also defined. Once the parameters for each working condition have

been set, you can proceed to submit the task for solution and calculation. As depicted in Fig. 5, each diagram displays the cloud map representing the distribution of equivalent stress in the rolling deformation zone.

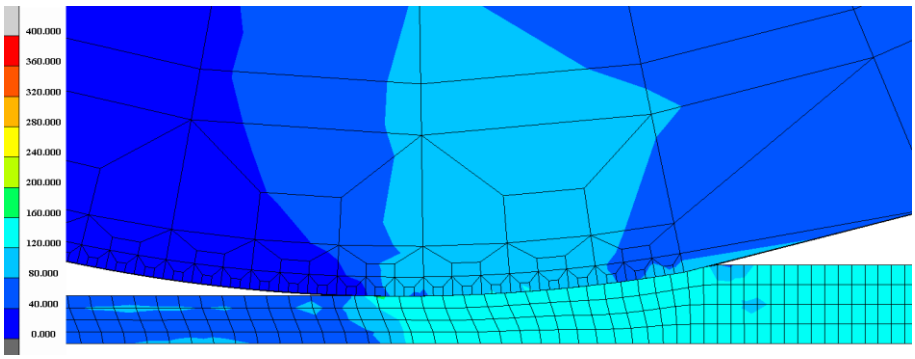

a) First frame

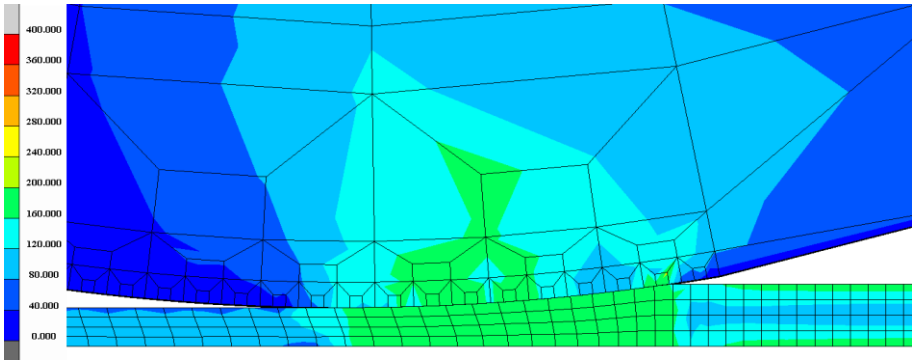

b) Second frame

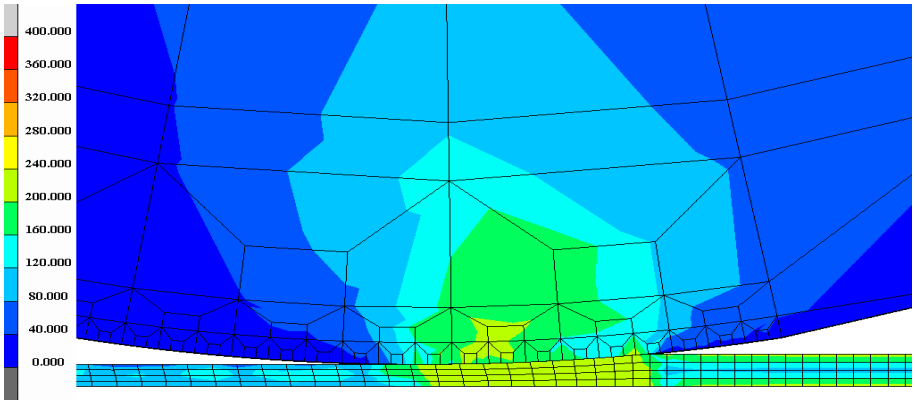

c) Third frame

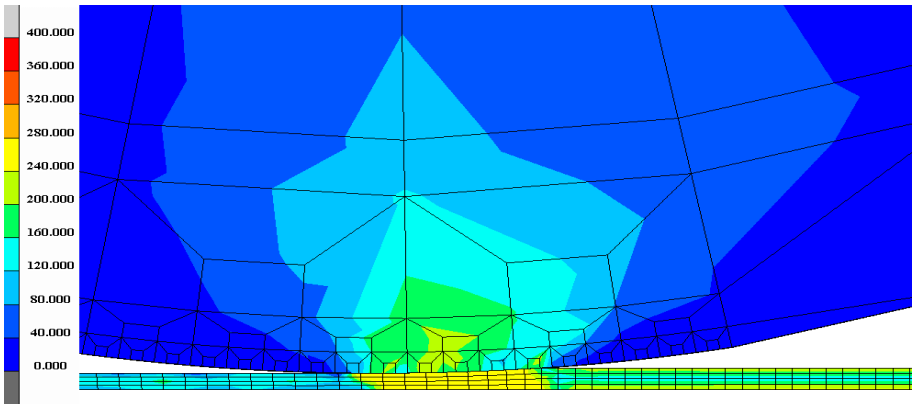

d) Forth frame

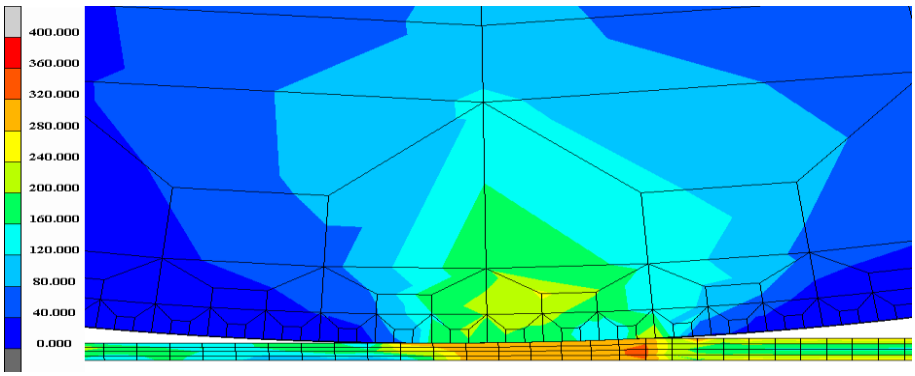

e) Fifth frame

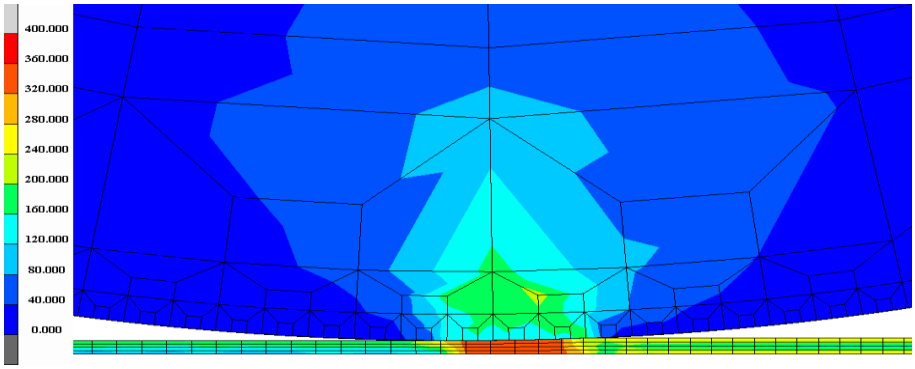

f) Sixth frame

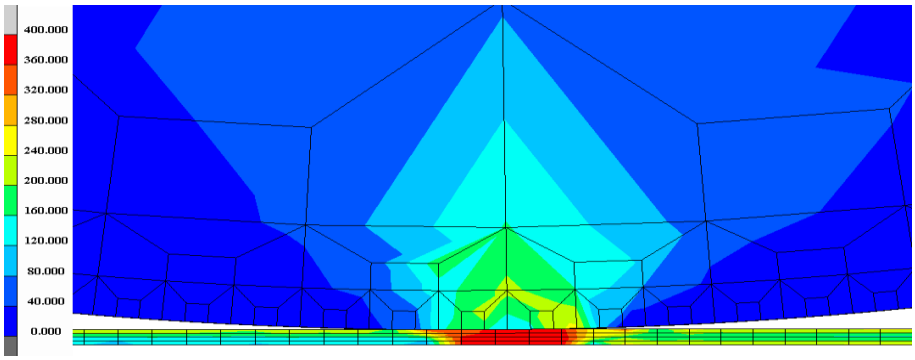

g) Seventh frame

Figure 5: Stress distribution status in deformation zone of each frame during rolling process.

Fig. 5 displays the stress distribution cloud map for each frame's deformation zone during the 700 L rolling process of beam steel. The data in the figure reveals a progressive increase in stress within the deformation zones as rolling continues. Specific data is presented in Table III, allowing us to conclude that as the strip becomes thinner, its deformation resistance steadily rises. Despite a notable reduction in the reduction rate of the 6th and 7th frames, the internal Mises stress within the strip steel's deformation zone is on the rise.

Table III: Statistics of equivalent stress in the deformation zone of rolled parts of each frame.

Rack number	1#	2#	3#	4#	5#	6#	7#
Equivalent stress (MPa)	160	200	210	260	330	360	370

4.2 Thickness distribution of strip steel in rolling deformation zone

After completing the finite element simulation process, we obtained lateral distribution data for the strip steel's thickness as it passes through the rolling deformation zone of each frame.

Subsequently, these thickness lateral distribution data were extracted, and we utilized Origin software to create curves, allowing us to visualize the changes in thickness distribution as the strip steel progresses through the first to the seventh stand.

Based on the horizontal distribution cloud map of thickness within the deformation zone of each frame and the outlet thickness distribution curve, it is evident that, along the width of the plate, the thickness of the strip steel remains relatively stable in the central area, with only a slight decrease in thickness observed at the edges.

4.3 Optimization of rolling process parameters

Furthermore, to validate the accuracy of the finite element simulation, three consecutive rolling trials were conducted using identical incoming materials and process parameters. On-site measurements of the outlet strip thickness were taken for the 5^{th}, 6^{th}, and 7^{th} stands. Table IV below presents a comparison between the finite element simulation results for the centre thickness of the outlet strip and the corresponding measured values.

Table IV: Simulation values and measured values for the centre thickness of export strip steel.

Rack number	**1#**	**2#**	**3#**	**4#**	**5#**	**6#**	**7#**
Finite element simulation thickness value (mm)	28.02	17.130	11.520	8.765	6.805	5.740	5.277
Measured value (mm)	—	—	—	—	7.03	5.97	5.51
Error (%)	—	—	—	—	3.20	3.85	4.23

Table IV demonstrates that the deviation between the outlet strip thickness, as simulated using the finite element method, and the actual measured value remains within 5 %. This substantiates the accuracy of our finite element simulation. Moreover, examining the thickness distribution curve reveals a consistent trend. Beginning from the outlet of the second frame, the transverse distribution of strip steel thickness exhibits an increase in the central region. This trend continues through the third, fourth, and fifth frames, where this characteristic intensifies. By the time we reach the outlet of the sixth frame, there is a significant abnormal increase in middle thickness of the strip steel. Although the issue of excessive middle thickness at the outlet of the seventh frame has been partly alleviated, it remains unresolved.

Due to the small bending force of each frame, the force between the rolling roller and the strip steel is large on both sides and small in the middle, resulting in the problem of thick and thin strip steel in the middle. It is possible to compensate for the compression of the middle part of the strip steel by appropriately increasing the bending force of the previous several frames. Based on the results and combined with the actual production situation on site, it is analysed that the uneven lateral distribution of the finished strip thickness of the hot continuous rolling unit is due to only paying attention to the adjustment of the bending and shifting rolls of the last three stands, while neglecting the parameter adjustment of the first four stands. In this way, during rolling, it will occur that the thickness of the strip steel has exceeded the tolerance in the first four stands, and due to the influence of work hardening, the thickness distribution of the strip steel in the last three stands cannot be effectively adjusted.

Therefore, the optimized rolling process parameters were used for experiments on the production site. The optimized bending force and roll displacement are shown in Table V. Without changing other process parameters, the thickness distribution of the finished strip steel was observed and measured. Fig. 6 shows the physical image of the finished strip steel before and after parameter optimization, and Fig. 7 shows the measured average thickness distribution curve of the finished strip steel before and after parameter optimization.

Table V: The table of optimized bending force and roll displacement parameters.

Rack number	**1#**	**2#**	**3#**	**4#**	**5#**	**6#**	**7#**
Work roll bending force (kN)	750	750	750	750	650	650	650
Work roll displacement (mm)	20	20	20	20	20	20	20

a)

b)

Figure 6: Comparison diagram of finished strip steel before and after parameter optimization; a) before parameter optimization, b) after parameter optimization.

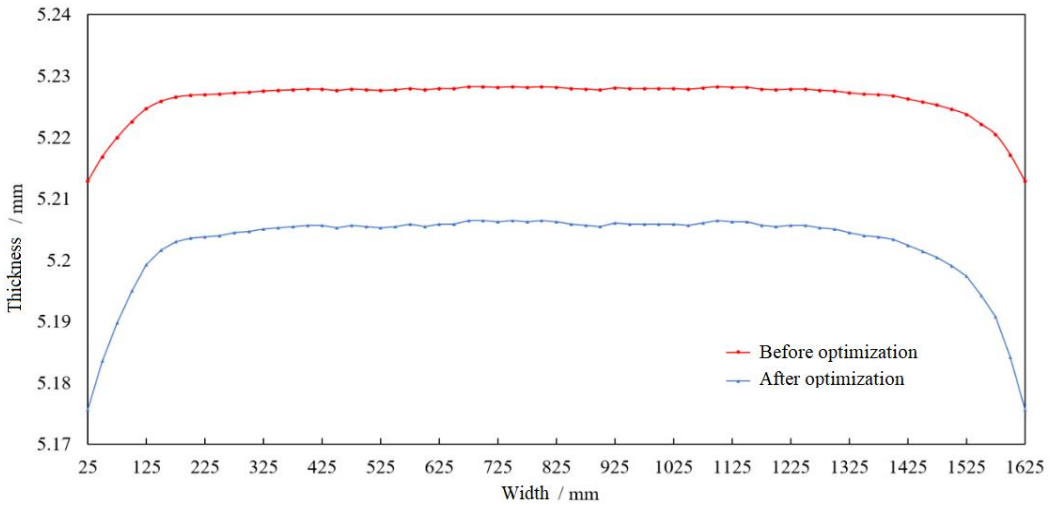

Figure 7: Distribution curve of average thickness of finished strip steel before and after optimization.

It can be seen from Fig. 6, the finished strip steel showed edge waves before optimization, that is, the thickness of the edge of the strip steel was thinner, and after optimization, the finished strip steel was straighter. It is intuitive to see that the transverse distribution of the optimized strip steel thickness is more uniform.

As seen from Fig. 7, the thickness difference of finished strip steel C45 before and after optimization has been reduced by 60 %, the uniformity of transverse thickness distribution has been effectively improved, and the defects of thickness exceeding the tolerance have been solved, proving the practicality and effectiveness of the research described in this article.

5. CONCLUSION

To effectively improve the quality of the finished strip steel of the seven stand hot rolling mill and reveal the relationship between the process parameters of each stand and the distribution of outlet thickness during the rolling process, this study used finite element simulation to simulate the stress and strain of the rolls and strip steel during the rolling process of the seven stand hot rolling mill. The genetic law of the transverse thickness distribution of the strip steel during the rolling process was studied, and the thickness deviation defect was solved by adjusting the process parameters. The main conclusions were as following:

(1) The accuracy of finite element simulation is demonstrated by comparing the measured strip steel thickness data at the outlet of each rack on site with the simulated data, and the errors are all within 5 %.

(2) The significant thickness deviations at the exit of the finished strip steel begin to emerge from the second frame, and become most obvious in the sixth frame. Although the uneven distribution of strip steel thickness is alleviated by adjusting process parameters in the seventh frame, the thickness deviation of the strip steel is still too large.

(3) According to the results obtained from finite element simulation, by adjusting the bending force and roll displacement of the first four frames, the thickness difference of the finished strip steel C45 is reduced by 60 %, and the defect of lateral thickness exceeding the tolerance of the strip steel is solved.

The established model is more accurate and closer to the actual production on site, and has important guiding significance for the optimization of the hot continuous rolling mill process and the study of the problem of excessive lateral thickness of strip steel.

ACKNOWLEDGEMENT

This work was supported by the Hebei Provincial Science and Technology Research and Development Plan – Science and Technology Support Plan project (23280101Z), the Hebei Provincial Higher Education Science and Technology Research Project (CXY2023012), the Hebei Provincial Major Science and Technology Achievement Transformation Project (22281001Z), the Liaoning Provincial Department of Education Higher Education Basic Project (LJKZZ20220040), and the Central Guiding Local Science and Technology Development Fund project (236Z1024G).

REFERENCES

[1] Chashchin, V. V. (2020). Substantiation for the implementation of controlled coil cooling technology after hot rolling of strip steel, *Steel in Translation*, Vol. 50, No. 8, 559-566, doi:10.3103/S0967091220080033

[2] Bolobanova, N. L.; Kotov, K. A.; Yusupov, V. S. (2023). Study and prediction of plasticization of hot-rolled steel strip during straightening under conditions of alternating deformation, *Metallurgist*, Vol. 66, No. 10, 1290-1298, doi:10.1007/s11015-023-01443-1

[3] Mimoune, D.; Zaaf, M.; Amirat, A. (2022). Contribution to improving hydrodynamics method for hot strip rolling application, *The International Journal of Advanced Manufacturing Technology*, Vol. 122, No. 9-10, 4165-4178, doi:10.1007/s00170-022-10042-4

[4] Platov, S. I.; Dema, R. R.; Latypov, O. R.; Banshchikov, V. S.; Mustafin, V. A.; Kharchenko, M. V.; Terent'ev, D. V. (2021). Effect of the temperature-speed hot-rolling conditions on scale formation, *Russian Metallurgy (Metally)*, Vol. 2021, No. 13, 1766-1770, doi:10.1134/S0036029521130231

[5] Prinz, K.; Steinboeck, A.; Müller, M.; Ettl, A.; Schausberger, F.; Kugi, A. (2019). Online parameter estimation for adaptive feedforward control of the strip thickness in a hot strip rolling mill, *Journal of Manufacturing Science and Engineering*, Vol. 141, No. 7, Paper 071005, 12 pages, doi:10.1115/1.4043575

[6] Schindler, I.; Hadasik, E.; Kopeček, J.; Kawulok, P.; Fabik, R.; Opela, P.; Rusz, S.; Kawulok, R.; Jablonska, M. (2015). Optimization of laboratory hot rolling of brittle Fe-40at.%Al-Zr-B aluminide, *Archives of Metallurgy and Materials*, Vol. 60, No. 3, 1693-1701, doi:10.1515/amm-2015-0293

[7] Chai, X.-J.; Li, H.-B.; Zhang, J.; Zhong, Y.-Z.; Ma, H.-H.; Zhang, P.-W. (2018). Flatness analysis and control of strips with different thickness in 2250 mm hot tandem rolling, *Steel Research International*, Vol. 89, No. 12, Paper 1800404, 10 pages, doi:10.1002/srin.201800404

[8] Qi, H.-P.; Li, H.-B.; Shuai, M.-R.; Wang, Q. (2023). Calculation and evolution of rolling force for hot rolled steel plate, *Heavy Machinery*, Vol. 2023, No. 2, 97-102, doi:10.13551/j.cnki.zxjxqk.2023.02.008

[9] Linghu, K.-Z.; Qiu, Z.-B.; Zhang, Y.-D.; Kuang, S.; Zhang, Y.-Y. (2023). Development of evaluation technology for flatness control capability of bending roll of hot rolling mill, *Steel Rolling*, Vol. 40, No. 3, 18-22, doi:10.13228/j.boyuan.issn1003-9996.20230303

[10] Liu, Y.; Wang, X.-J.; Sun, J.; Liu, G.-M.; Li, H.-Y.; Ji, Y.-F. (2023). Strip thickness and profile-flatness prediction in tandem hot rolling process using mechanism model-guided machine learning, *Stell Research International*, Vol. 94, No. 1, Paper 2200447, doi:10.1002/srin.202200447

[11] Liu, X.; Xiao, H. (2020). Theoretical and experimental study on the producible rolling thickness in ultra-thin strip rolling, *Journal of Materials Processing Technology*, Vol. 278, Paper 116537, 9 pages, doi:10.1016/j.jmatprotec.2019.116537

[12] Gu, H.-G.; Zhang, D.-W.; Zhang, Q.; Sun, L.; Luo, B. (2022) Analysis of factors influencing the thickness of hot rolled strip head, *Hebei Metallurgy*, Vol. 2022, No. 9, 64-67, doi:10.13630/j.cnki.13-1172.2022.0914

[13] Ma, X.-B.; Wang, D.-C.; Liu, H.-M.; Zhang, S. (2019). Influence of profile indicators of hot-rolled strip on transverse thickness difference of cold-rolled silicon steel, *Metallurgical Research & Technology*, Vol. 116, No. 1, Paper 105, 15 pages, doi:10.1051/metal/2018044

[14] Hu, Y.-J.; Sun, J.; Chen, S. Z.; Zhang, X.; Peng, W.; Zhang, D.-H. (2020). Optimal control of tension and thickness for tandem cold rolling process based on receding horizon control, *Ironmaking & Steelmaking*, Vol. 47, No. 6, 606-616, doi:10.1080/03019233.2019.1615813

[15] Zeng, W.-Y.; Wang, J.-K.; Zhang, Y.; Han, Y.-H.; Zhao, Q. (2022). DDPG-based continuous thickness and tension coupling control for the unsteady cold rolling process, *The International Journal of Advanced Manufacturing Technology*, Vol. 120, No. 11-12, 7277-7292, doi:10.1007/s00170-022-09239-4

[16] Liu, K.; Wang, X.-C.; Zhang, T.-M.; He, H.-Z. (2023). Analysis of wedge control in hot strip rolling based on finite element simulation, *China Metallurgy*, Vol. 2023, No. 9, 104-111, doi:10.13228/j.boyuan.issn1006-9356.20230295

[17] Luo, T.; Wang, S.-R.; Zhang, C.-G.; Liu, X.-L. (2017). Parameters deterioration rules of surrounding rock for deep tunnel excavation based on unloading effect, *DYNA*, Vol. 92, No. 6, 648-654, doi:10.6036/8554

[18] Wang, S. R.; Xiao, H. G.; Zou, Z. S.; Cao, C.; Wang, Y. H.; Wang, Z. L. (2019). Mechanical performances of transverse rib bar during pull-out test, *International Journal of Applied Mechanics*, Vol. 11, No. 5, Paper 1950048, 15 pages, doi:10.1142/S1758825119500480

[19] Liu, G. F.; Cui, X. Y.; Li, Z. Z.; Wang, J. H.; Zhang, X. D.; Bai, Z. H. (2022). Shape change simulation analysis of wheel steel in a four-high hot rolling mill, *International Journal of Simulation Modelling*, Vol. 21, No. 4, 603-614, doi:10.2507/IJSIMM21-4-621